The Cryosphere Discuss., https://doi.org/10.5194/tc-2019-28
Manuscript under review for journal The Cryosphere
Discussion started: 22 February 2019

Changing Characteristics of Runoff and Freshwater Export From Watersheds Draining Northern Alaska

Michael A. Rawlins[1], Lei Cai[2], Svetlana L. Stuefer[3], and Dmitry Nicolsky[4]

[1]Department of Geosciences, University of Massachusetts, Amherst, MA 01003, USA
[2]International Arctic Research Center, University of Alaska Fairbanks, Fairbanks, AK 99775
[3]Civil and Environmental Engineering, College of Engineering and Mines, University of Alaska Fairbanks, Fairbanks, AK 99775 USA
[4]Geophysical Institute, University of Alaska Fairbanks, Fairbanks, AK 99775, USA

Corresponding author: Michael A. Rawlins <rawlins@geo.umass.edu>

Abstract

The quantity and quality of river discharge in arctic regions is influenced by many processes including climate, watershed attributes and, increasingly, hydrological cycle intensification and permafrost thaw. We used a hydrological model to quantify baseline conditions and investigate the changing character of hydrological elements for Arctic watersheds between Point Barrow and just west of Mackenzie River over the period 1981–2010. The region annually exports 28.1 km^3 yr^{-1} of freshwater via river discharge, with 51.9% (14.6 km^3 yr^{-1}) coming collectively from the Colville, Kuparuk, and Sagavanirktok rivers. Our results point to significant ($p < 0.05$) increases (134–212% of average) in cold season discharge (CSD) for several large North Slope rivers including the Colville and Kuparuk, and for the region as a whole. A significant increase

The Cryosphere Discuss., https://doi.org/10.5194/tc-2019-28
Manuscript under review for journal The Cryosphere
Discussion started: 22 February 2019

in the proportion of subsurface runoff to total runoff is noted for the region and 24 of 42 study basins, with the change most prevalent across the northern foothills of the Brooks Range. Relatively large increases in simulated active-layer thickness (ALT) suggest a physical connection between warming climate, permafrost degradation, and increasing subsurface flow to streams and rivers. A decline in terrestrial water storage (TWS) is attributed to losses in soil ice that outweigh gains in soil liquid water storage. Over the 30 yr period the timing of peak spring (freshet) discharge shifts earlier by 4.5 days, though the time trend is only marginally ($p = 0.1$) significant. These changing characteristics of Arctic rivers have important implications for water, carbon, and nutrient cycling in coastal environments.

KEYWORDS: Arctic; runoff; river discharge; permafrost

1 Introduction

The arctic water cycle is central to a range of climatic processes and to the transfer of carbon, energy, and a host of other constituents from the land mass to coastal waters of the Arctic Ocean. Freshwater export to the Arctic Ocean is high relative to the ocean's area (Shiklomanov et al., 2000), and dominated by river discharge (Serreze et al., 2006), which serves as a conveyance for carbon and heat across the land-ocean boundary. Syntheses of data and models have advanced understanding of key linkages and feedbacks in the Arctic system (Francis et al., 2009), mean freshwater budgets across the land, atmosphere and ocean domains (Serreze et al., 2006), and time trends in observations and model estimates over the latter decades of the 20^{th} century (Rawlins et al., 2010).

A warming climate is expected to lead to intensification of the hydrological cycle, including increases in net precipitation (P) at high latitudes. Evidence pointing to Arctic hydrological cycle intensification is emerging (Peterson et al., 2002, 2006; Rawlins et al., 2010; Zhang et al., 2013; Bring et al., 2016). A more vigorous cycle is related both to the amount of moisture air can hold and changes in atmospheric dynamics. Much of the increase in net P is expected to occur during winter (Kattsov et al., 2007), potentially through intensified local surface evaporation driven by retreating winter sea ice, and enhanced moisture inflow from lower latitudes (Zhang et al., 2013; Bintanja and Selten, 2014). An increase in river discharge from Eurasia to the Arctic Ocean was noted in simulations with the HadCM3 general circulation model (Wu et al., 2005), illustrating the potential for increased winter net P to influence freshwater export. Positive trends in column-integrated precipitable water over the region north of 70°N, linked to positive anomalies in air and sea surface temperature and negative anomalies in end-of-summer sea ice extent (Serreze et al., 2012), support the future model projections. Rivers form a primary conduit for transferring terrestrial materials to the coastal ocean, and these materials exert a strong influence on marine ecosystems and carbon processing.

Permafrost warming and degradation has been observed over parts of Alaska, Russia, and Canada (Brown and Romanovsky, 2008; Romanovsky et al., 2010; Smith et al., 2010). In one study permafrost area is projected to decrease by more than 40%, assuming climate stablization at 2°C above pre-industrial (Chadburn et al., 2017). Warming and permafrost degradation is expected to cause a shift in arctic environments from a surface water-dominated system to a groundwater-dominated system (Frey and McClelland, 2009; Bring et al., 2016). There is increasing evidence of impacts of permafrost degradation on biogeochemical cycles on land and in aquatic systems. Recent reported increases in baseflow in arctic rivers are suggestive of increased hydrological conductivity due to permafrost thaw (Walvoord and Striegl, 2007; Bense et al., 2009; St. Jacques and Sauchyn, 2009). Groundwater processes have a dominant role in controlling carbon export from the land to streams in permafrost terrain (Frey and McClelland, 2009; Neilson et al., 2018). Dissolved organic matter (DOM) transported by Arctic rivers contain geochemical signatures of the watersheds they drain, reflecting their unique characteristics (Kaiser et al., 2017). Changes in landscape characteristics and water flow paths as a result of climatic warming and associated active layer thickening have the potential to alter aquatic and riverine biogeochemical fluxes (Frey and McClelland, 2009; Wrona et al., 2016; Wickland et al., 2018). Increased flow through mineral soils has been linked to decreases in DOC export from the Yukon River over recent decades (Striegl et al., 2005). In contrast, areas with deep peat deposits that experience thaw may see increasing DOC mobilization and export as permafrost degrades (Frey and Smith, 2005).

This study presents baseline freshwater flux estimates and examines elements of the hydrological cycle across the North Slope over the period 1981–2010. We use measured data to assess model performance and quantify freshwater export from the region. We then leverage the modeling framework to investigate signs of change in runoff and river discharge, the proportion of groundwater runoff, terrestrial water storage, and the timing of peak daily discharge. Salient results in the context of arctic change and directions for future research are discussed.

The Cryosphere Discuss., https://doi.org/10.5194/tc-2019-28
Manuscript under review for journal The Cryosphere
Discussion started: 22 February 2019

2 Study Area, Data and Modeling

Our study focuses on the North Slope of Alaska and far NW Canada, partitioned by the region's river basins that drain to the Beaufort Sea and Arctic Ocean. In the text, we refer to the entire study area as the "North Slope". Model input and output fields are resolved at a daily time step. The grid is based on the Northern Hemisphere EASE-Grid (Brodzik and Knowles, 2002), with a horizontal resolution of 25 km for each cell. The area draining the North Slope contains 312 grid cells (total area = 196,060 km^2) across northern Alaska and extreme northwest Canada. It is defined by the watersheds (42 in total) of rivers with an outlet along the coast from just west of the Mackenzie River to Utqiakvik (formerly Barrow) to the west. Hydrologic modeling was performed for 42 watersheds. Many North Slope rivers are oriented roughly north-south. The study area is underlain by continuous permafrost, approximately 250–300 m thick in the Brooks Range and, locally, up to nearly 400 m thick near the coast (Jorgenson et al., 2008).

2.1 Observational data

Observational data used in this study include time series of daily river discharge, end-of-winter snow water equivalent (SWE), and seasonal maximum active-layer thickness (ALT). Historical river discharge data for the Kuparuk River (station 15896000) was retrieved from the USGS at http://waterdata.usgs.gov/nwis/uv?15896000. Simulated ALT from the PWBM (section 2.3) is compared with estimates from a related high-resolution 1-D heat conduction model (developed by the University of Alaska's Geophysical Institute Permafrost Laboratory, hereafter referred to as GIPL) that incorporated data on ecosystem type and was validated against measured CALM network ALTs (Nicolsky et al., 2017). Model simulated SWE is evaluated against average values from 12 years of SWE observations collected across a 200×300 km domain that includes the Kuparuk River watershed from the Brooks Range to the Beaufort Sea coast (Stuefer et al., 2013).

2.2 Reanalysis data

Gridded fields of daily surface (2 m) air temperature, precipitation (P), and wind speed are used as model forcings. Obtaining accurate temporally varying P estimates at daily resolution is particular challenging in arctic environments. Gauge undercatch of solid P is common, the gauge network is sparse and the number of stations at higher elevation is insufficient (Yang et al., 1998, 2005; Kane and Stuefer, 2015). In this study model meteorological forcings are drawn from the Modern-Era Retrospective Analysis for Research and Applications (MERRA; Rienecker et al. (2011)). In a recent intercomparison of P estimates over the Arctic Ocean and its peripheral seas, three reanalyses— ERA-Interim (Dee et al. (2011)), MERRA, and NCEP R2 (Kistler et al. (2001))— produce realistic magnitudes and temporal agreement with observed P events, while two products (MERRA, version 2 (MERRA-2), and CFSR) show large, implausible magnitudes in P events (Boisvert et al., 2018). Given a modest low bias in monthly P across the North Slope in MERRA, we derived a new bias corrected daily P time series by scaling the MERRA values by a factor defined using monthly long-term mean P (1981–2010) from MERRA, ERA-Interim, and a data set that blends simulations from ERA-Interim and the Polar WRF (Cai et al., 2018). Those three data sets exhibit a similar spatial pattern in annual P across the region. Annual P generally ranges from as low as 200 mm yr^{-1} near the coast to over 400 mm yr^{-1} over the foothills of the Brooks Range. At each grid cell, the offset ratio was defined as average P from the 3 data sets divided by the MERRA P amount. The derived daily P (hereafter MERRA*) was then calculated as the daily MERRA P amount multiplied by the offset ratio.

2.3 Hydrological modeling

The regional hydrology is characterized by water fluxes and storages expressed in simulations using a spatially-distributed numerical model. Referenced previously as the Pan-Arctic Water Balance Model (PWBM), the numerical framework encompasses all major elements of the water cycle, including snow storage, sublimation, transpiration, and surface evaporation (Rawlins et al., 2003, 2013). It is run at an implicit daily time step and is typically forced with meteorological data. The PWBM has been used to investigate causes behind the record Eurasian discharge in 2007 (Rawlins et al., 2009); to corroborate remote sensing estimates of surface water dynamics (Schroeder et al., 2010); and to quantify present and future water cycle changes in the area of Nome, Alaska (Clilverd et al., 2011). In a comparison against observed river discharge, PWBM-simulated SWE fields compared favorably (Rawlins et al., 2007). Soil temperature dynamics are simulated through a 1-D nonlinear heat conduction model with phase change (Rawlins et al., 2013; Nicolsky et al., 2017). PWBM includes a multi-layer snow model that accounts for wind compaction, change in density due to fresh snowfall, and depth hoar development with time. Runoff is the sum total of surface (overland) and subsurface flow each day. Subsurface runoff occurs when the amount of water in a soil layer exceeds field capacity.

The model is well suited for application across the North Slope region. Active-layer thickness (ALT) simulated using the PWBM soil submodel was found to be more similar to in situ observations and airborne radar retrievals in continuous permafrost areas than in lower permafrost probability areas (Yi et al., 2018). The influence of snow cover and soil thermal dynamics on the seasonal and spatial variability in soil CO_2 respiration was quantified by coupling PWBM to a dynamic soil carbon model (Yi et al., 2013, 2015). A key model attribute is its ability to dynamically simulate the direct influence the snowpack exerts on soil temperature (Yi et al., 2019), with deeper snowpacks promoting warmer soils and associated effects, such as enhancement of soil decomposition and respiration from deeper ($\geq$ 0.5 m) soil layers (Yi et al., 2015).

In this study we applied an updated version of the model, and given its detailed representation of soil freeze-thaw processes, rename it the "Permafrost Water Balance Model" (hereafter PWBM v3). Modifications involved the incorporation of new data and parametrizations for surface fractional open water (fw) cover, soil carbon content, and transient ponded surface evaporation and runoff. Updates to the spatial estimates of f_w were taken from a product derived from brightness temperature (T_b) retrievals from the Advanced Microwave Scanning Radiometer for EOS (AMSR-E) (Du et al., 2017) to parameterize the grid cell fraction of open water (annual average) across the model domain. Properties of near surface organic-rich soils strongly control hydrological and thermal dynamics in the seasonally thawed active layer. We used soil organic carbon (SOC) estimates from version 2.2 of the Northern Circumpolar Soil Carbon Database (NCSCD), a digital soil map database linked to extensive field-based SOC storage data (Hugelius et al., 2014). The database contains SOC stocks for the upper 0–1 m and for deeper soils from 1–2 and 2–3 m depth. In the updated PWBM v3 the sum total of SOC in the upper 3 m was used to derive the organic layer thickness as described in Rawlins et al. (2013). The resulting spatially varying parameterizations of soil carbon profiles (% of volume) with depth over the domain (Figure S1b) influence soil thermal properties and hydrological storages and fluxes. The maps show broad agreement in the spatial pattern of the independent soil texture and soil carbon datasets. Sandy soils and soil carbon thicknesses under 20 cm occur over the Brooks Range, and relatively higher soil carbon thicknesses and loam soils are present across the tundra to the north. Following initial assessments we increased soil carbon amounts by 10% in areas of sandy soils and reassigned 24 grid cells to loam, to be more consistent with soil textures inferred from the high-resolution ALT mapping via the GIPL model that incorporated data on ecosystem type (Nicolsky et al., 2017).

Parameters controlling evaporation and runoff fluxes from transient surface storages were modified to better account for delays in water reaching stream channels.

Defining E_i, R_i, and S_i to represent evaporation (or evapotransipration)(mm day^{-1}), runoff (mm day^{-1}, and storage (mm) in soil layer i, respectively, then E_0, R_0, S_0 are evaporation, runoff, and storage from the model surface layer, $R_0 = S_0 * f$ (mm day^{-1}). In the updated model f = 0.40, reduced from the prior value of 0.75. Evaporation from surface storage is $E_0 = S_0 * g$, with g now reduced to 1/3 of the potential ET rate.

Model estimated runoff routed through a simulated topological network (STN) (Vörösmarty et al., 2000) is expressed as river discharge (volume flux) at the coastal outlets of 42 individual watersheds draining from Point Barrow to just west of the Mackenzie River delta. A simple linear routing model is used given the relatively short travel times through the North Slope basins. Water transferred to the downstream grid (or ocean/lagoon) is

$$Q_{out} = \frac{v}{d} S \qquad (1)$$

where Q_{out} (m^3 s^{-1}) is flow downstream, v is flow velocity (m s^{-1}), d is the distance between grid cells (m), and S is volume of river water (m^3). Miller et al. (1994) suggested a global average of $v = 0.35$ m s^{-1}. Given the relatively flat topography over much of the domain we set effective velocity at $v = 0.175$.

The model is run in a 50 year spinup over year 1980 prior to the transient time series simulation to stabilize soil temperature and water storage pools. This spinup is followed by a 30 year transient simulation over the period 1981–2010, the focus of our analysis.

Statistical significance of a time trend in runoff or river discharge is assessed using the Mann-Kendall test statistic (Hamed and Rao, 1998; Yue et al., 2002), with a 95% confidence level ($p < 0.05$) designated as statistically significant. A General Linear Model (GLM) is assumed for other analyzed quantities. A one or a two-sided test is applied depending on whether the direction of change is assumed. For example, we posit null hypotheses that the region is experiencing increasing cold season discharge as a result of ALT increase. Percent change over time is estimated using the GLM linear least squares slope and the climatological average for the time series examined.

3 Results

3.1 Active layer thickness

Simulated maximum seasonal ALT derived from daily soil temperatures in the updated PWBM v3 model run using the MERRA (bias corrected MERRA* P) display the expected north-south gradient which reflects the gradient in summer (and

The Cryosphere Discuss., https://doi.org/10.5194/tc-2019-28
Manuscript under review for journal The Cryosphere
Discussion started: 22 February 2019

annual) air temperature. The pattern is also evident in ALT predicted from the GIPL, with agreement strongest in coastal areas. The fields differ near the center of the domain where the PWBM produces relatively lower ALT compared to GIPL. Area averaged ALT from PWBM and GIPL is 53.5 and 55.2 cm respectively, a difference of ∼3% (Table 1). The differences increase toward the extremes of each field, pointing to larger spatial variability in the PWBM simulations. ALT from simulations with the default MERRA P forcing are shallower and less in agreement with the GIPL data.

3.2 Snow water equivalent

Within the Kuparuk basin maximum end of season SWE typically occurs near the end of April. Model simulated (PWBM v3) end of season SWE each year is calculated as the average of daily values from April 24 to May 7, also averaged across all basin grids. The model SWE largely tracks the interannual variations in measured end of season SWE over the period 2000–2010, with an average difference of 5.3 mm or 4.8% of the average (109.7 mm) from the field measurements (Figure S3). The Pearson correlation efficient is $r = 0.78$, with the relationship significant at $p < 0.01$ (Figure S4).

3.3 Runoff and river discharge

3.3.1 Spring freshet

Modeled spring freshet runoff (R) is evaluated against observed R for the Kuparuk River watershed. USGS measurements for the Kuparuk River at Deadhorse over the period 1981–2010 show that an average of 98.3 mm of runoff (R) is exported as discharge during the spring freshet, which we calculate as R occurring from day of year (DOY) 100 to 180. R is the unit depth of discharge over a given time interval, and distributed over a contributing watershed. Modeled freshet R calculated from the simulation forced with MERRA* leads the observed freshet R by approximately 10 days. This despite a relatively slow model river flow velocity (v = 0.175 m^3 s^{-1}). Simulated R over the freshet period is 98.0 mm. Simulated May R exceeds observed R by 29 mm month^{-1}, while simulated June R is 29 mm month^{-1} lower than observed R (Figure 1), resulting in the relatively small error (percent difference +0.3%) for total R over the freshet period. Simulated R closely tracks observed R in other months of the year with flow.

3.3.2 Annual runoff and freshwater export

Annual total P over the Kuparuk Basin ranges from 182 mm yr^{-1} (2007) to 433 mm yr^{-1} (2003) with no significant trend over the 30 year period (Figure 2). For annual total R the long-term average from USGS observations and from the model simulation are 144 and 134 mm yr^{-1}, respectively (percent difference = −6.8%). There is no significant trend in observed or simulated annual R over the 30 yr period. Simulated annual R is correlated with observed annual R (Pearson correlation $r = 0.74$, $p < 0.001$), with average error of +3.1 mm yr^{-1} (Figure S5). Observed R varies from 75–238 mm yr^{-1}, while simulated R is more conservative, extending over a range from 90–200 mm yr^{-1}. In other words, the model tends to overestimate R in years with low annual flow, and vice versa. For measured R partitioned at: $R < 100$ mm yr^{-1}, $100 \leq R \leq 200$ mm yr^{-1}, and $R > 200$ mm yr^{-1}, average errors are +24.5, −1.8, and −52.2 mm yr^{-1}, respectively. It is notable that in both 1996 and 2003, annual R is higher in the year following a peak (within a several year span) in annual P. This lag highlights the role that antecedent storage plays in the region's river discharge regimes and is consistent with previous research (Bowling et al., 2003; Stuefer et al., 2017). The spatial pattern in annual R (Figure 3a) reflects a similar gradient in annual P from the coast southward into the Brooks Range, as R is largely controlled by P and snow accumulation variations across the region. R averages over 250 mm yr^{-1} across parts of the Brooks Range, while coastal areas average under 50 mm yr^{-1}.

In the modeling framework simulated R is routed along the gridded river network and expressed as a volume flux of river discharge (Q) at the Beaufort Sea coast. For the period 1981–2010, annual total Q for the Colville, Kuparuk, and Sagavanirktok rivers combined averages 14.57 km^3 yr^{-1}, which is 51.9% of the North Slope domain total annual Q of 28.10 km^3 yr^{-1} (Table 2). Those 3 watersheds occupy 46.2% of the North Slope study domain.

3.3.3 Cold season discharge (CSD)

Cold season (Nov–Apr) discharge (CSD) from the region (0.116 km^3 season^{-1}) is 0.4% of annual total Q, and between 0.2–0.3% for each of the Colville, Kuparuk, and Sagavanirktok rivers. In this region nearly all of the CSD occurs during the first half of winter, namely November and December. CSD for the entire North Slope basin, and both the Colville and Kuparuk rivers, increased significantly (Mann-Kendall test, $p < 0.05$, Table 2, Figure 4). The CSD increase from the Colville is 215% of the long-term average. For the North Slope basin as a whole CSD increased 134% of the long-term average. Increasing CSD is noted for 9.0% of the North Slope domain, and 28.4% of the Colville basin, primarily in headwater catchments of the foothills of the Brooks Range (Figure 3b). In total the affected terrain covers 88,601 km^2 or 45% of the North Slope drainage.

3.4 Fraction of subsurface runoff

We examine variations in modeled surface and subsurface R through the year to better understand how warming is altering the hydrological flows. For the region as a whole the fraction of subsurface runoff to total runoff (hereafter (F_{sub}) increased 4.4% (p$<$ 0.01), a 31% change relative to the 30 yr average of 14%. Both the Colville and Sagavanirktok rivers show statistically significant ($p < 0.05$) increases in F_{sub}, as do 20 of the 40 remaining basins. Significant increases are noted during several months, most widespread in September (58 of 312 grids or 18.6% of region) (Figure 5). Conversely, July shows a decrease in F_{sub}, although over less total area (5.4%). For June and September the F_{sub} increases average 34.8 and 40.2% respectively for the total change over the period. For July the average is −38.3%, with 17 grids showing an increase and two a decrease. At the annual scale the increase in F_{sub} is significant ($p < 0.05$) for 24.7% of the study domain, most notably across the northern foothills of the Brooks Range from the western part of the region (Colville basin) eastward and toward the coast (Figure 6). F_{sub} is consistently 100% of total runoff after October. Areas with increasing F_{sub} are co-located with the areas experiencing increasing CSD.

Increasing F_{sub} is noted in areas with a significant increase in active-layer thickness (ALT), primarily across parts of the northern foothills of the Brooks Range and the smaller basins near 140°W longitude (Figure 7). The simulation shows that one fifth of the region (20.2%) experienced a significant increase in both F_{sub} and ALT ($p <$ 0.05, Table 3). A fraction of the foothills region (5.1% of domain) is characterized by a positive trend in F_{sub} only. Statistically significant increases in ALT are widespread (66.7%). The ALT trend average for grid cells with a significant increase in F_{sub} only, a significant increase in ALT only, and a significant increase in both are 0.17, 0.75, and 1.00 cm yr^{-1}, respectively. The relatively high ALT increases in areas of significant F_{sub} increase indicate a connection between increased thaw and subsurface water flow in those areas (Figure 8, Table 3).

3.5 Terrestrial water storage

Terrestrial water storage (TWS) over a given time interval is defined by the total amount of water stored in snow, soil liquid water, and soil ice estimated by the model. Over the 1981–2010 period annual average TWS (all 312 domain grids) ex-

The Cryosphere Discuss., https://doi.org/10.5194/tc-2019-28
Manuscript under review for journal The Cryosphere
Discussion started: 22 February 2019

hibits a negative trend of approximately -2 mm yr^{-1} ($p < 0.001$, Figure 9). Declines in annual minimum (-1.7 mm yr^{-1}) and maximum TWS (-2.3 mm yr^{-1}) are also significant. Among the component storages there is no significant change in snow storage, an increase in minimum soil water amounts, and a decrease in soil ice (Figure S6). The -2 mm yr^{-1} decrease in TWS reflects a decrease in soil ice of -2.5 mm yr^{-1}, a (insignificant) decrease in snow of -0.16 mm yr^{-1}, and an increase in soil water storage of 0.61 mm yr^{-1}. In addition to the annual averages, significant increases (decreases) in soil water (ice) annual minimum and maximum amounts are also noted.

3.6 Timing of maximum discharge

Warming and associated changes in snowmelt have the potential to cause shifts in the timing of peak discharge (Q) during the spring freshet period. Maximum spring discharge is determined from the daily routed Q for each of the 42 North Slope river basins. In the model simulation only one of the 42 basins exhibits a significant shift to earlier maximum daily Q. None show a significant shift to later maximum Q. The average date of maximum daily Q across the 42 basin advanced by approximately 4.5 days (Figure S7), though the change is not statistically significant ($p = 0.1$). Maximum daily Q from the region in recent years occurs near DOY 150 (end of May), though this estimate is potentially biased 8–10 days early based on the comparison of simulated runoff with measurements for the Kuparuk River (subsection 3.3).

4 Summary and Discussion

Recent studies have investigated how hydrological cycle intensification and permafrost thaw may alter terrestrial hydrological fluxes and, in turn, materials exports to coastal zones. Changes unfolding across high latitude watersheds have the potential to significantly alter water, carbon, and other constituent fluxes, with implications for nearshore Arctic biogeochemical and ecological processes.

Simulated runoff from PWBM v3 shows peak spring discharge that is systematically 8–10 days early relative to gauge data. This bias is unrelated to river flow velocity in the PWBM routing scheme, and more likely due to a combination of errors in air temperature forcing (warm bias) that lead to early snowpack thaw, and/or insufficient surface storages in the mode which would delay the transfer of water to stream networks. Simulated R timing may improve by better accounting for these delays in snowmelt runoff. Future studies should investigate how dynamic surface inundation data being produced from microwave and radar remote sensing (Schroeder et al., 2010; Du et al., 2016) can be used to constrain surface water storage, its partitioning to runoff and evaporation, and flow direction in areas of low topographic relief. The lag in runoff in 1996 and 2003 highlight how precipitation and antecedent storage conditions can influence the following year's runoff (Bowling et al., 2003; Stuefer et al., 2017).

The quantity and quality of freshwater export is expected to change significantly as the Arctic hydrological cycle intensifies and the system transitions toward increasing groundwater water flows (Frey et al., 2003; Frey and McClelland, 2009). In this study evidence of change is evident in cold season discharge from the North Slope region over the 30 year period examined. There is no significant trend in annual total discharge. However, we note that the Kuparuk and nearby Putuligayuk River experienced high annual runoff in 2013, 2014, and 2015 (Stuefer et al., 2017), consistent with expectations under an intensifying arctic hydrological cycle (Wu et al., 2005; Rawlins et al., 2010). Climate models project a future increase in Arctic precipitation that is generally greatest in autumn and winter and smallest in summer, and greatest over the higher latitudes of Eurasia and North America (ACIA, 2005; Kattsov et al., 2007). Higher winter snowfall amounts are possible over the North Slope, which may, in turn, lead to higher freshwater discharges. Though relatively small in magnitude, the simulation produces an increase in cold season discharge of 134% and 215% of the long-term average for the North Slope and Colville basins, respectively. Basins showing a significant increase in cold season discharge cover 45% of the region. Within the Colville basin the change is being driven by processes in headwater subbasins of the northern foothills and mountains of the Brooks Range (Figure 3b). Landscape conditions in those areas strongly influences the quality of water exported during the first half of winter, including the solubility, chemical character, and biodegradability of carbon, nitrogen and other nutrients (Wickland et al., 2018). Mobilization of water through permafrost thaw has been identified as factor in the observed rise in winter (low flow) discharge in parts of the Arctic (St. Jacques and Sauchyn, 2009; Smith et al., 2007; Walvoord and Striegl, 2007). As with the results of the present study, observed increase in winter discharge and decrease in the ratio of maximum to minimum monthly discharge in the middle and lower part of the Lena River basin reflect the controls permafrost exerts on winter discharge (Gautier et al., 2018).

Our results also show changes in the proportion of groundwater runoff for the region as a whole, and individually the Colville, Sagavanirktok, and 22 of the other 42 river basins. Increases are noted across the foothills and higher elevations of the northern Brooks Range. The growing subsurface flows are contributing to the in-

The Cryosphere Discuss., https://doi.org/10.5194/tc-2019-28
Manuscript under review for journal The Cryosphere
Discussion started: 22 February 2019

creasing cold season discharge amounts, with the most significant changes in both quantities found across headwaters of several of the larger basins (Colville and Sagavanirktok), as well as areas near the coast east of approximately 140°W. Increases in both subsurface runoff and cold season discharge are very likely manifestations of climate warming, as active layer thaw depths are highly responsive to warming air temperatures (Hinkel and Nelson, 2003). Approximately 20% of the region, the Brooks Range foothills and smaller watersheds near 140°W, shows significant increases in both the fraction of subsurface runoff and active layer thickness. The active layer increase is greatest in those areas experiencing growing subsurface runoff contributions, suggesting a direct connection between thawing soils and changing subsurface flows. A deepening active layer associated with climate warming will very likely lead to a longer unfrozen period in deeper soils (Yi et al., 2019), enhancing subsurface runoff flow. A larger thawed zone permits additional water storage that supports runoff in late autumn, before soils freeze completely. Diffuse lateral groundwater flow at the land-water boundary in coastal regions can exerts a strong influence on nearshore geochemistry, relative to surface streamflows, in some areas.

The changes captured in the modeling are consistent with the notion that permafrost thaw enhances hydrogeologic connectivity and increases low flows in permafrost regions (Bense et al., 2009, 2012; Bring et al., 2016; Lamontagne-Hallé et al., 2018). Evidence of permafrost thaw and increasing groundwater flow has been reported in recent studies using measurements from arctic rivers. Recent increases in nitrate concentrations and export from the Kuparuk River are consistent with permafrost degradation and deepening flow paths (McClelland et al., 2007). 'Old' carbon measured in Arctic rivers indicates mobilization of pre-industrial organic matter and subsequent transfer to rivers. (Schuur et al., 2009; Mann et al., 2015; Dean et al., 2018). St. Jacques and Sauchyn (2009) concluded that increases in winter baseflow and mean annual streamflow in the NWT were caused predominately by climate warming via permafrost thawing that enhances infiltration and deeper flowpaths and hydrological cycle intensification (Frey and McClelland, 2009; Bring et al., 2016). The magnitude of the groundwater runoff change in the present simulations should be viewed with caution given the intrinsic resolution of model parameterizations for soil texture, organic layer thickness, and other landscape properties. Our results, however, do point to a close correspondence between active layer thickness and subsurface runoff increases across the foothills of the Brooks Range. This result suggests that the relatively thin surface organic layer and sandy soils in the foothills areas may be seeing a relative larger impact on soil warming and thaw. Consistent with our results, a study using PWBM in a satellite-based modeling framework found that ALT deepening across much of the Brooks Range has been greater than in the tundra to the north (Yi et al., 2018).

Consistent with recent warming and associated ALT increases, our results suggest an overall decline (-2 mm yr^2) in terrestrial water storage across the North Slope drainage basin over the 1981–2010 period. This decrease is driven by losses in soil ice, with an increase in liquid water storage which does not fully offset the ice losses. With continued warming it is likely that the timing of snowmelt will advance, with impacts to the timing of peak (maximum daily) spring discharge. Averaged across all 42 basins, the date of daily maximum discharge advanced 4.5 days over the 1981–2010 period, though the change is not statistically significant ($p = 0.1$) at the 95% confidence level. Individual river basins show larger and more significant shifts to earlier maximum dicharge. Future changes toward earlier peak discharge can be expected given projections of future warming.

Modeling studies of the impacts of climate warming on permafrost thaw and groundwater discharge are key to our understanding of lateral hydrological flows and associated constituent exports. Given uncertainties in solid precipitation amounts results of this study should be corroborated through evaluation of simulations produced with alternate forcings and through parameter sensitivity analysis. A fuller understanding of the extent of water cycle alterations in this region will require new measurements of storage and flux terms along with continued development of numerical models which capture the important role ground ice plays in runoff generating processes. New discharge observations outside of the freshet period, and in ungaged basins, and associated geochemical sampling can be useful to partition surface and groundwater amounts. Regarding linkages with biogeochemical fluxes, water samples from the mouths of major Arctic river show that dissolved organic carbon in those rivers is sourced primarily from fresh vegetation during the two month of spring freshet and from older, soil-, peat-, and wetland-derived DOC during groundwater dominated low flow conditions (Amon et al., 2012). Stable isotope data obtained from river water samples can be used to guide partitioning of surface and groundwater water flows to better understand how soil drainage and soil moisture redistribution will change with future permafrost thaw and ALT deepening (Walvoord and Kurylyk, 2016).

High performance computing is shedding insights into hydrological flows and biogeochemical cycling (Lamontagne-Hallé et al., 2018; Neilson et al., 2018). Improvements in numerical model simulations of groundwater flow regimes in permafrost areas have helped to shed insight on the important roles that microtopography and soil properties play in groundwater runoff regimes. Model calibration and validation for simulations at finer spatial scales is dependent on new field measurements of parameters such as water table height, active layer thickness, and soil organic carbon content with depth. Simulations for future conditions in the region should take into account processes directly influenced by permafrost thaw (Bense et al., 2012; Lamontagne-Hallé et al., 2018). To overcome challenges in deriving parameterization from multiple disparate data sets, high-resolution ecosystem maps of the Alaska North Slope can provide a convenient upscaling mechanism to parameterize ground soil properties across the region (Nicolsky et al., 2017). Given its considerable effect on soil thermal and hydraulic properties, modeling efforts will benefit from improved mapping of soil organic matter. Measurements and modeling of fluvial biogeochemistry can also help shed insight on changing watershed characteristics influencing water quantity, quality, and associated land-ocean exports.

5 Acknowledgments

M.A.R acknowledges support from the U.S. National Science Foundation, Office of Polar Programs (NSF-OPP-1656026) and U.S. Department of Energy (DE-SC0019462). The authors thank Jinyang Du for assistance with the surface fractional open water product and Raymond Bradley, John Kimball, and James McClelland for comments on an earlier version of the manuscript. Model outputs and code from this study are available at:
`http://www.geo.umass.edu/climate/data/NSdata.html`

6 Author Contributions

M.A.R designed the study, executed the model simulations, and performed the analysis. L.C, S.L.S., and D.N. contributed data. M.A.R drafted the initial manuscript and all authors contributed to its development and publication.

Competing interests: The authors declare that they have no conflict of interest.

The Cryosphere Discuss., https://doi.org/10.5194/tc-2019-28
Manuscript under review for journal The Cryosphere
Discussion started: 22 February 2019

References

ACIA: *Arctic Climate Impact Assessment*, 1042 pp., Cambridge University Press, New York, 2005. 12

Amon, R., Rinehart, A., Duan, S., Louchouarn, P., Prokushkin, A., Guggenberger, G., Bauch, D., Stedmon, C., Raymond, P., Holmes, R., et al.: Dissolved organic matter sources in large Arctic rivers, Geochimica et Cosmochimica Acta, 94, 217–237, 2012. 14

Bense, V., Ferguson, G., and Kooi, H.: Evolution of shallow groundwater flow systems in areas of degrading permafrost, Geophysical Research Letters, 36, 2009. 3, 13

Bense, V. F., Kooi, H., Ferguson, G., and Read, T.: Permafrost degradation as a control on hydrogeological regime shifts in a warming climate, J. Geophys. Res., 117, doi:10.1029/2011JF002143, 2012. 13, 15

Bintanja, R. and Selten, F. M.: Future increases in Arctic precipitation linked to local evaporation and sea-ice retreat, Nature, 509, 479–482, doi:http://dx.doi.org/10.1038/nature13259 10.1038/nature13259, 2014. 2

Boisvert, L. N., Webster, M. A., Petty, A. A., Markus, T., Bromwich, D. H., and Cullather, R. I.: Intercomparison of Precipitation Estimates over the Arctic Ocean and Its Peripheral Seas from Reanalyses, Journal of Climate, 31, 8441–8462, doi:10.1175/JCLI-D-18-0125.1, URL `https://doi.org/10.1175/JCLI-D-18-0125.1`, 2018. 5

Bowling, L. C., Kane, D. L., Gieck, R. E., Hinzman, L. D., and Lettenmaier, D. P.: The role of surface storage in a low-gradient Arctic watershed, Water Resources Research, 39, 2003. 9, 12

Bring, A., Fedorova, I., Dibike, Y., Hinzman, L., Mård, J., Mernild, S., Prowse, T., Semenova, O., Stuefer, S. L., and Woo, M.-K.: Arctic terrestrial hydrology: A synthesis of processes, regional effects, and research challenges, Journal of Geophysical Research: Biogeosciences, 121, 621–649, 2016. 2, 3, 13

Brodzik, M. J. and Knowles, K.: EASE-Grid: A Versatile Set of Equal-Area Projections and Grids, in M. Goodchild (Ed.) Discrete Global Grids. Santa Barbara, CA, USA: National Center for Geographic Information and Analysis., 2002. 4

Brown, J. and Romanovsky, V. E.: Report from the International Permafrost Association: State of permafrost in the first decade of the 21st century, Permafrost Periglacial Proc., 19, 255–260, 2008. 3

Cai, L., Alexeev, V. A., Arp, C. D., Jones, B. M., Liljedahl, A. K., and Gädeke, A.: The Polar WRF Downscaled Historical and Projected Twenty-First Century Climate for the Coast and Foothills of Arctic Alaska, Frontiers in Earth Science, 5, 111, doi:10.3389/feart.2017.00111, URL `https://www.frontiersin.org/article/10.3389/feart.2017.00111`, 2018. 5

Chadburn, S., Burke, E., Cox, P., Friedlingstein, P., Hugelius, G., and Westermann, S.: An observation-based constraint on permafrost loss as a function of global warming, Nature Climate Change, 7, 340, 2017. 3

Clilverd, H. M., White, D. M., Tidwell, A. C., and Rawlins, M. A.: The Sensitivity of Northern Groundwater Recharge to Climate Change: A Case Study in Northwest Alaska, Journal of the American Water Resources Association, pp. 1–13, 2011. 5

Dean, J., van der Velde, Y., Garnett, M. H., Dinsmore, K. J., Baxter, R., Lessels, J. S., Smith, P., Street, L. E., Subke, J.-A., Tetzlaff, D., et al.: Abundant pre-industrial carbon detected in Canadian Arctic headwaters: implications for the permafrost carbon feedback, Environmental Research Letters, 13, 034 024, 2018. 13

Dee, D. P., Uppala, S. M., Simmons, A., Berrisford, P., Poli, P., Kobayashi, S., Andrae, U., Balmaseda, M., Balsamo, G., Bauer, d. P., et al.: The ERA-Interim reanalysis: Configuration and performance of the data assimilation system, Quarterly Journal of the royal meteorological society, 137, 553–597, 2011. 5

Du, J., Kimball, J. S., Jones, L., and Watts, J. D.: Implementation of satellite based fractional water cover indices in the pan-Arctic region using AMSR-E and MODIS, Remote Sensing of Environment, 184, 469–481, 2016. 12

Du, J., Kimball, J. S., Duguay, C., Kim, Y., and Watts, J. D.: Satellite microwave assessment of Northern Hemisphere lake ice phenology from 2002 to 2015, The Cryosphere, 11, 47, 2017. 6

Francis, J. A., Cassano, J. J., Gutowski Jr., W. J., Hinzman, L. D., Holland, M. M., Steele, M. A., White, D. M., and Vörösmarty, C. J.: An Arctic Hydrologic System in Transition: Feedbacks and Impacts on Terrestrial, Marine, and Human Life, J. Geophys. Res., 114, G04019, doi:10.1029/2008JG000902, 2009. 2

Frey, K. E. and McClelland, J. W.: Impacts of permafrost degradation on arctic river biogeochemistry, Hydrol. Processes, 23, 169–182, doi:10.1002/hyp.7196, 2009. 3, 12, 13

Frey, K. E. and Smith, L. C.: Amplified carbon release from vast West Siberian peatlands by 2100, Geophysical Research Letters, 32, doi:10.1029/2004GL022025, URL http://dx.doi.org/10.1029/2004GL022025, 2005. 3

Frey, K. E., McClelland, J. W., Holmes, R. M., and Smith, L. C.: Impacts of climate warming and permafrost thaw on the riverine transport of nitrogen and phosphorus to the Kara Sea, J. Geophys. Res., 112, g04S58, DOI:10Ð1029/2006JG000369, 2003. 12

Gautier, E., Dépret, T., Costard, F., Virmoux, C., Fedorov, A., Grancher, D., Konstantinov, P., and Brunstein, D.: Going with the flow: Hydrologic response of middle Lena River (Siberia) to the climate variability and change, Journal of Hydrology, 557, 475–488, 2018. 12

Hamed, K. H. and Rao, A. R.: A modified Mann-Kendall trend test for autocorrelated data, Journal of hydrology, 204, 182–196, 1998. 7

Hinkel, K. and Nelson, F.: Spatial and temporal patterns of active layer thickness at Circumpolar Active Layer Monitoring (CALM) sites in northern Alaska, 1995–2000, Journal of Geophysical Research: Atmospheres, 108, 2003. 13

Hugelius, G., Strauss, J., Zubrzycki, S., Harden, J. W., Schuur, E., Ping, C.-L., Schirrmeister, L., Grosse, G., Michaelson, G. J., Koven, C. D., et al.: Estimated stocks of circumpolar permafrost carbon with quantified uncertainty ranges and identified data gaps, Biogeosciences, 11, 6573–6593, 2014. 6

Jorgenson, M., Yoshikawa, K., Kanevskiy, M., Shur, Y., Romanovsky, V., Marchenko, S., Grosse, G., Brown, J., and Jones, B.: Permafrost characteristics of Alaska, in: Proceedings of the Ninth International Conference on Permafrost, vol. 3, pp. 121–122, University of Alaska: Fairbanks, 2008. 4

Kaiser, K., Canedo-Oropeza, M., McMahon, R., and Amon, R. M.: Origins and transformations of dissolved organic matter in large Arctic rivers, Scientific reports, 7, 13 064, 2017. 3

Kane, D. and Stuefer, S.: Reflecting on the status of precipitation data collection in Alaska: a case study, Hydrol Res., 46, 478–493, 2015. 4

The Cryosphere Discuss., https://doi.org/10.5194/tc-2019-28
Manuscript under review for journal The Cryosphere
Discussion started: 22 February 2019

Kattsov, V. M., Walsh, J. E., Chapman, W. L., Govorkova, V. A., Pavlova, T. V., and Zhang, X.: Simulation and Projection of Arctic Freshwater Budget Components by the IPCC AR4 Global Climate Models, J. Hydrometeorol., 8, 571–589, doi:10.1175/JHM575.1, 2007. 2, 12

Kistler, R., Kalnay, E., Collins, W., Saha, S., White, G., Woolen, J., Chelliah, M., Ebisuzaki, W., Kanamitsu, M., Kousky, V., van den Dool, H., Jenne, R., and Fiorino, M.: The NCEP-NCAR 50-year reanalysis: Monthly means CD-ROM and documentation, Bull. Am. Meteorol. Soc., 82, 247–267, 2001. 5

Lamontagne-Hallé, P., McKenzie, J. M., Kurylyk, B. L., and Zipper, S. C.: Changing groundwater discharge dynamics in permafrost regions, Environmental Research Letters, 13, 084 017, URL http://stacks.iop.org/1748-9326/13/i=8/a=084017, 2018. 13, 14, 15

Mann, P. J., Eglinton, T. I., McIntyre, C. P., Zimov, N., Davydova, A., Vonk, J. E., Holmes, R. M., and Spencer, R. G.: Utilization of ancient permafrost carbon in headwaters of Arctic fluvial networks, Nature communications, 6, 2015. 13

McClelland, J. W., Stieglitz, M., Pan, F., Holmes, R. M., and Peterson, B. J.: Recent changes in nitrate and dissolved organic carbon export from the upper Kuparuk River, J. Geophys. Res., 112, g04S60, doi:10.1029/2006JG000371, 2007. 13

Miller, J. R., Russell, G. L., and Caliri, G.: Continental-scale river flow in climate models, Journal of Climate, 7, 914–928, 1994. 7

Neilson, B. T., Cardenas, M. B., O'Connor, M. T., Rasmussen, M. T., King, T. V., and Kling, G. W.: Groundwater Flow and Exchange Across the Land Surface Explain Carbon Export Patterns in Continuous Permafrost Watersheds, Geophysical Research Letters, 0, doi:10.1029/2018GL078140, URL https://agupubs.onlinelibrary.wiley.com/doi/abs/10.1029/2018GL078140, in press, 2018. 3, 14

Nicolsky, D. J., Romanovsky, V., Panda, S., Marchenko, S., and Muskett, R.: Applicability of the ecosystem type approach to model permafrost dynamics across the Alaska North Slope, Journal of Geophysical Research: Earth Surface, 122, 50–75, 2017. 4, 5, 6, 15, 2

Peterson, B. J., Holmes, R. M., McClelland, J. W., Vörösmarty, C. J., Lammers, R. B., Shiklomanov, A. I., Shiklomanov,

The Cryosphere Discuss., https://doi.org/10.5194/tc-2019-28
Manuscript under review for journal The Cryosphere
Discussion started: 22 February 2019

I. A., and Rahmstorf, S.: Increasing river discharge to the Arctic Ocean, Science, 298, 2171–2173, doi:10.1126/science.1077445, http://www.sciencemag.org/content/298/5601/2171.short, 2002. 2

Peterson, B. J., McClelland, J., Curry, R., Holmes, R. M., Walsh, J. E., and Aagaard, K.: Trajectory shifts in the Arctic and sub-Arctic freshwater cycle, Science, 313, 1061–1066, doi:10.1126/science.1122593, http://www.sciencemag.org/content/313/5790/1061.short, 2006. 2

Rawlins, M., Nicolsky, D., McDonald, K., and Romanovsky, V.: Simulating soil freeze/thaw dynamics with an improved pan-Arctic water balance model, Journal of Advances in Modeling Earth Systems, 5, 659–675, doi:10.1002/jame.20045, URL http://dx.doi.org/10.1002/jame.20045, 2013. 5, 6

Rawlins, M. A., Lammers, R. B., Frolking, S., Fekete, B. M., and Vörösmarty, C. J.: Simulating Pan-Arctic Runoff with a Macro-Scale Terrestrial Water Balance Model, Hydrol. Processes, 17, 2521–2539, 2003. 5

Rawlins, M. A., Fahnestock, M., Frolking, S., and Vörösmarty, C. J.: On the Evaluation of Snow Water Equivalent Estimates over the Terrestrial Arctic Drainage Basin, Hydrol. Processes, 21, 1616–1623, dOI: 10.1002/hyp.6724, 2007. 5

Rawlins, M. A., Serreze, M. C., Schroeder, R., Zhang, X., and McDonald, K. C.: Diagnosis of the Record Discharge of Arctic-Draining Eurasian Rivers in 2007, Environ. Res. Lett., 4, 045011, doi: 10.1088/1748-9326/4/4/045011, 2009. 5

Rawlins, M. A., Steele, M., Holland, M. M., Adam, J. C., Cherry, J. E., Francis, J. A., Groisman, P. Y., Hinzman, L. D., Huntington, T. G., Kane, D. L., and Coauthors: Analysis of the Arctic System for Freshwater Cycle Intensification: Observations and Expectations, J. Clim., 23, 5715–5737, doi:http://dx.doi.org/10.1175/2010JCLI3421.1, http://journals.ametsoc.org/doi/abs/10.1175/2010JCLI3421.1, 2010. 2, 12

Rienecker, M., Suarez, M., Gelaro, R., Todling, R., Bacmeister, J., Liu, E., Bosilovich, M., Schubert, S., Takacs, L., Kim, G., et al.: MERRA-NASA's Modern-Era Retrospective Analysis for Research and Applications, Bulletin of the American Meteorological Society, 2011. 5

Romanovsky, V. E., Smith, S. L., and Christiansen, H. H.: Permafrost thermal state in the polar Northern Hemisphere during the international polar year 2007–2009:

The Cryosphere Discuss., https://doi.org/10.5194/tc-2019-28
Manuscript under review for journal The Cryosphere
Discussion started: 22 February 2019

a synthesis, Permafrost Periglacial Proc., 21, 106–116, doi:10.1002/ppp.689, URL http://dx.doi.org/10.1002/ppp.689, 2010. 3

Schroeder, R., McDonald, K. C., Zimmerman, R., Podest, E., and Rawlins, M.: North Eurasian Inundation Mapping with Passive and Active Microwave Remote Sensing, Environ. Res. Lett., 5, 015003, doi:10.1088/1748-9326, 2010. 5, 12

Schuur, E., Vogel, J. G., Crummer, K. G., Lee, H., Sickman, J. O., and Osterkamp, T. E.: The effect of permafrost thaw on old carbon release and net carbon exchange from tundra, Nature, 459, 556–559, 2009. 13

Serreze, M. C., Barrett, A. P., Slater, A. G., Woodgate, R. A., Aagaard, K., Lammers, R. B., Steele, M., Moritz, R., Meredith, M., and Lee, C. M.: The large-scale freshwater cycle of the Arctic, J. Geophys. Res., 111, doi:10.1029/2005JC003424, http://onlinelibrary.wiley.com/doi/10.1029/2005JC003424/full, 2006. 2

Serreze, M. C., Barrett, A. P., and Stroeve, J.: Recent changes in tropospheric water vapor over the Arctic as assessed from radiosondes and atmospheric reanalyses, Journal of Geophysical Research: Atmospheres (1984–2012), 117, doi:10.1029/2011JD017421, 2012. 3

Shiklomanov, I. A., Shiklomanov, A. I., Lammers, R. B., Peterson, B. J., and Vörösmarty, C. J.: The dynamics of river water inflow to the Arctic Ocean, pp. 281–296, Kluwer Academic Press, Dordrecht, in *The Freshwater Budget of the Arctic Ocean*, edited by E.I Lewis, et al., 2000. 2

Smith, L. C., Pavelsky, T. M., MacDonald, G. M., Shiklomanov, A. I., and Lammers, R. B.: Rising minimum daily flows in northern Eurasian rivers: A growing influence of groundwater in the high-latitude hydrologic cycle, J. Geophys. Res., 112, g04S47, doi:10.1029/2006JG000327, 2007. 12

Smith, S., Romanovsky, V., Lewkowicz, A., Burn, C., Allard, M., Clow, G., Yoshikawa, K., and Throop, J.: Thermal state of permafrost in North America: a contribution to the international polar year, Permafrost Periglacial Proc., 21, 117–135, doi:10.1002/ppp.690, URL http://dx.doi.org/10.1002/ppp.690, 2010. 3

St. Jacques, J. M. and Sauchyn, D. J.: Increasing winter baseflow and mean annual streamflow from possible permafrost thawing in the Northwest Territories, Canada, Geophys. Res. Lett., 36, L01401, doi:10.1029/2008GL035822, 2009. 3, 12, 13

The Cryosphere Discuss., https://doi.org/10.5194/tc-2019-28
Manuscript under review for journal The Cryosphere
Discussion started: 22 February 2019

Striegl, R. G., Aiken, G. R., Dornblaser, M. M., Raymond, P. A., and Wickland, K. P.: A decrease in discharge-normalized DOC export by the Yukon River during summer through autumn, Geophysical Research Letters, 32, doi:10.1029/2005GL024413, URL http://dx.doi.org/10.1029/2005GL024413, 2005. 3

Stuefer, S., Kane, D. L., and Liston, G. E.: In situ snow water equivalent observations in the US Arctic, Hydrology Research, 44, 21–34, 2013. 4, 3

Stuefer, S. L., Arp, C. D., Kane, D. L., and Liljedahl, A. K.: Recent Extreme Runoff Observations From Coastal Arctic Watersheds in Alaska, Water Resources Research, 53, 9145–9163, doi:10.1002/2017WR020567, URL https://agupubs.onlinelibrary.wiley.com/doi/abs/10.1002/2017WR020567, 2017. 9, 12

Vörösmarty, C. J., Fekete, B. M., Maybeck, M., and Lammers, R. B.: Gloabl System of Rivers: Its Role in Organizing Continental Land Mass and Defining Land-to-Ocean Linkages, Global Biogeochem. Cycles, 14, 599–621, 2000. 7

Walvoord, M. A. and Kurylyk, B. L.: Hydrologic impacts of thawing permafrost—A review, Vadose Zone Journal, 15, 2016. 14

Walvoord, M. A. and Striegl, R. G.: Increased groundwater to stream discharge from permafrost thawing in the Yukon River basin: Potential impacts on lateral export of carbon and nitrogen, Geophysical Research Letters, 34, 2007. 3, 12

Wickland, K. P., Waldrop, M. P., Aiken, G. R., Koch, J. C., Jorgenson, M. T., and Striegl, R. G.: Dissolved organic carbon and nitrogen release from boreal Holocene permafrost and seasonally frozen soils of Alaska, Environmental Research Letters, 13, 065 011, URL http://stacks.iop.org/1748-9326/13/i=6/a=065011, 2018. 3, 12

Wrona, F. J., Johansson, M., Culp, J. M., Jenkins, A., Mård, J., Myers-Smith, I. H., Prowse, T. D., Vincent, W. F., and Wookey, P. A.: Transitions in Arctic ecosystems: Ecological implications of a changing hydrological regime, Journal of Geophysical Research: Biogeosciences, 121, 650–674, 2016. 3

Wu, P., Wood, R., and Stott, P.: Human influence on increasing Arctic river discharges, Geophys. Res. Lett., 32, L02703, doi:10.1029/2004GL021570, 2005. 2, 12

The Cryosphere Discuss., https://doi.org/10.5194/tc-2019-28
Manuscript under review for journal The Cryosphere
Discussion started: 22 February 2019

Yang, D., Goodison, B. E., Ishida, S., and Benson, C. S.: Adjustment of Daily Precipitation Data at 10 Stations in Alaska: Application of World Meteorological Organization Intercomparison Results, Water Resour. Res., 34, 241–256, 1998. 4

Yang, D., Kane, D., Zhang, Z., Legates, D., and Goodison, B.: Bias corrections of long-term (1973–2004) daily precipitation data over the northern regions, Geophys. Res. Lett., 32, L19501, doi:10.1029/2005GL024057, 2005. 4

Yi, Y., Kimball, J. S., Jones, L. A., Reichle, R. H., Nemani, R., and Margolis, H. A.: Recent climate and fire disturbance impacts on boreal and arctic ecosystem productivity estimated using a satellite-based terrestrial carbon flux model, Journal of Geophysical Research: Biogeosciences, pp. 1–17, 2013. 6

Yi, Y., Kimball, J. S., Rawlins, M. A., Moghaddam, M., and Euskirchen, E. S.: The role of snow cover affecting boreal-arctic soil freeze/thaw and carbon dynamics, Biogeosciences, 12, 5811–5829, 2015. 6

Yi, Y., Kimball, J. S., Chen, R. H., Moghaddam, M., Reichle, R. H., Mishra, U., Zona, D., and Oechel, W. C.: Characterizing permafrost active layer dynamics and sensitivity to landscape spatial heterogeneity in Alaska, The Cryosphere, 12, 145–161, doi:10.5194/tc-12-145-2018, URL https://www.the-cryosphere.net/12/145/2018/, 2018. 6, 14

Yi, Y., Kimball, J. S., Chen, R. H., Moghaddam, M., and Miller, C. E.: Sensitivity of active-layer freezing process to snow cover in Arctic Alaska, The Cryosphere, 13, 197–218, doi:10.5194/tc-13-197-2019, URL https://www.the-cryosphere.net/13/197/2019/, 2019. 6, 13

Yue, S., Pilon, P., and Cavadias, G.: Power of the Mann–Kendall and Spearman's rho tests for detecting monotonic trends in hydrological series, Journal of hydrology, 259, 254–271, 2002. 7

Zhang, X., He, J., Zhang, J., Polyakov, I., Gerdes, R., Inoue, J., and Wu, P.: Enhanced poleward moisture transport and amplified northern high-latitude wetting trend, Nature Climate Change, 3, 47–51, doi:doi:10.1038/nclimate1631, 2013. 2

The Cryosphere Discuss., https://doi.org/10.5194/tc-2019-28
Manuscript under review for journal The Cryosphere
Discussion started: 22 February 2019

Table 1: Distribution statistics (cm) for spatial fields of active layer thickness (ALT) from the GIPL and PWBM simulation with MERRA* forcing shown in Figure S2. Also shown are statistics for a simulation using original (non-adjusted) MERRA precipitation (P) data.

Active Layer Thick Distribution Statistics (cm)					
Data	**5th**	**25th**	**mean**	**75th**	**95th**
GIPL	37.3	49.9	55.2	61.4	69.4
PWBM (MERRA)	30.5	40.3	50.4	58.6	75.2
PWBM (MERRA*)	32.0	43.7	53.5	61.3	79.0

Table 2: Basin area, annual discharge (Q), and cold season discharge (CSD) for several North Slope rivers and the full domain. Basins with a significant increase in CSD are indicated with a superscript *.

River Basin and Domain-Wide Discharge			
Basin	**Area (km^2)**	**Annual Q (km^3 yr^{-1})**	**CSD (km^3 season^{-1})**
Colville	64 095	10.21	0.023*
Kuparuk	10 054	1.35	0.004*
Sagavanirktok	16 338	3.01	0.006
3 River Total	90 487	14.57	0.032
North Slope	196 061	28.10	0.116*

Table 3: Number of grid cells, associated area fraction of domain, and average ALT and F_{sub} for each category shown. Domain consists of 312 grid cells spanning an area of 196,060.8 km^2.

Number of grids, area, and ALT and F_{sub} averages for each subregion.				
	N	**area (%)**	F_{sub} **(%^{3} yr^{-1})**	**ALT (cm yr^{-1})**
F_{sub} increase only	16	5.1	0.43	0.17
ALT increase only	211	67.6	0.05	0.75
both	63	20.2	0.35	1.00
neither	22	7.1	0.22	0.22

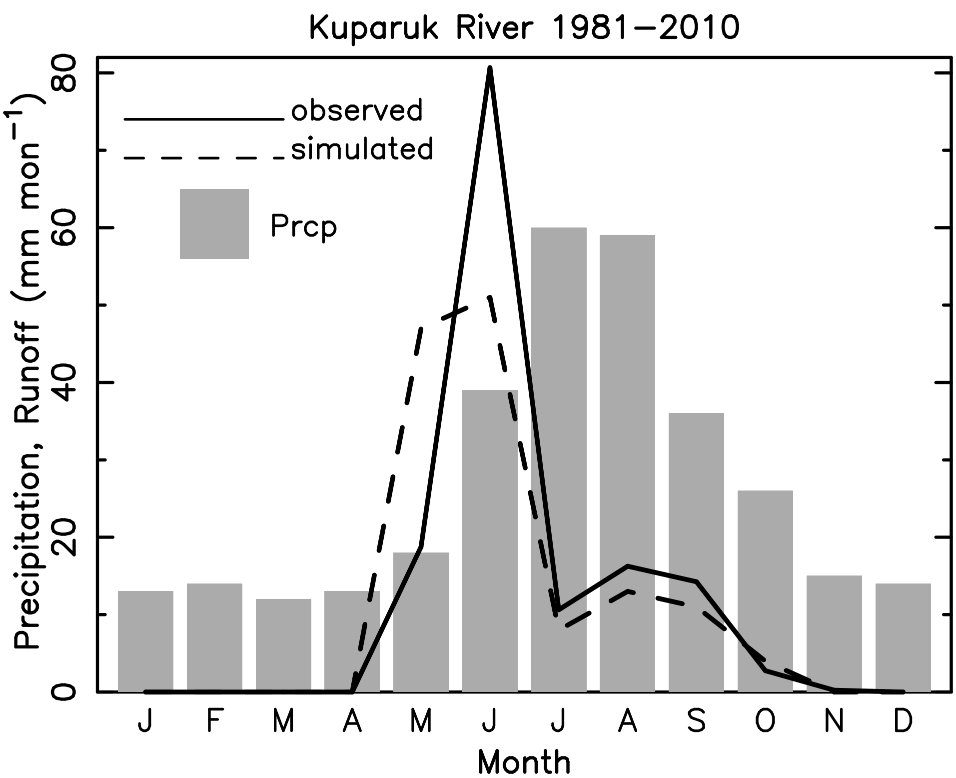

Figure 1: Monthly climatological precipitation (P) and simulated and observed runoff (R, mm month^{-1}) for the Kuparuk River basin 1981–2010. Simulated R expressed in unit depth was calculated from the routed river discharge (Q) volume Kuparuk. Forcing from the MERRA reanalysis, with precipitation adjustment (MERRA*) as described in section 2.2.

The Cryosphere Discuss., https://doi.org/10.5194/tc-2019-28
Manuscript under review for journal The Cryosphere
Discussion started: 22 February 2019

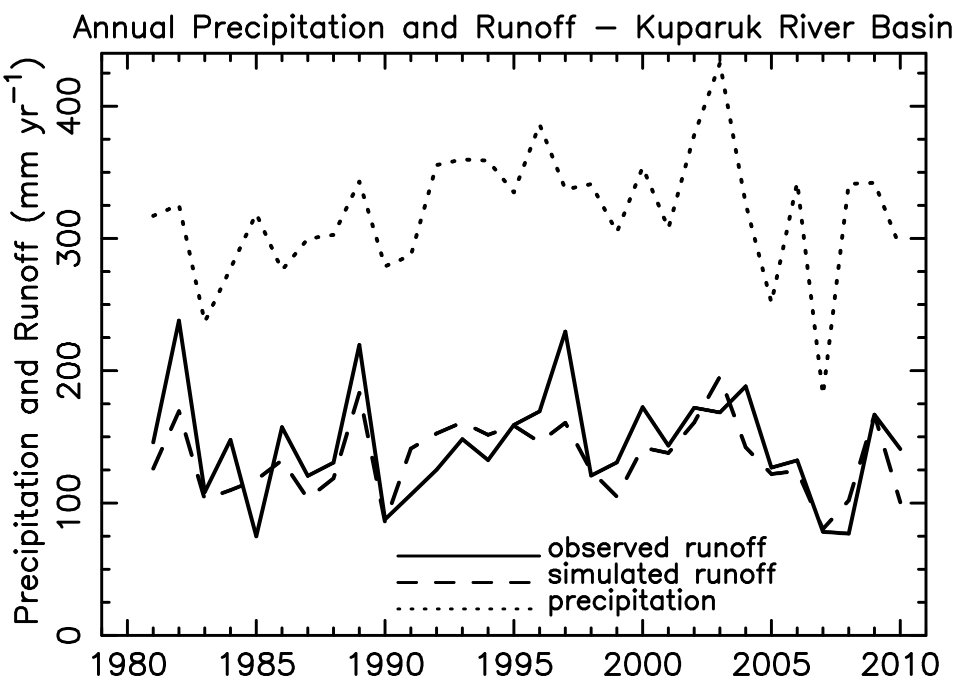

Figure 2: Annual total P from MERRA (adjusted) and simulated and observed R (mm yr^{-1}) over the Kuparuk basin for the simulation period 1981–2010.

The Cryosphere Discuss., https://doi.org/10.5194/tc-2019-28
Manuscript under review for journal The Cryosphere
Discussion started: 22 February 2019

The Cryosphere
Discussions

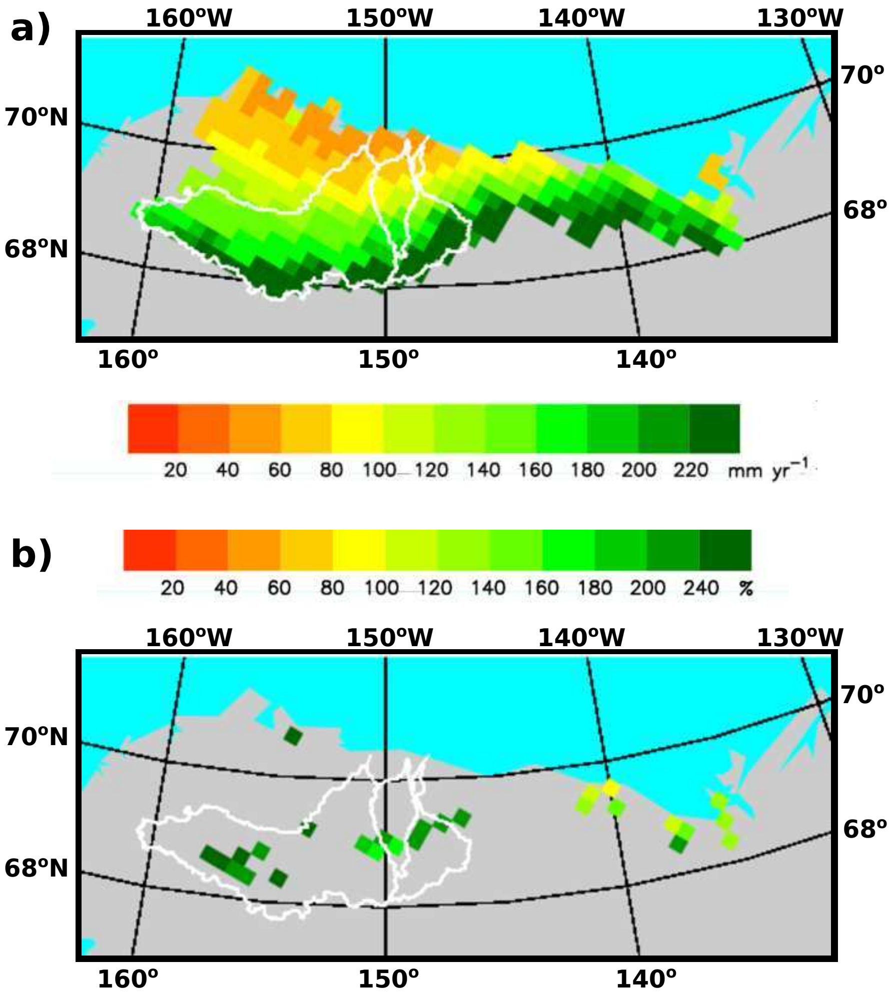

Figure 3: a) Annual total R 1981–2010 (mm yr^{-1}) from the model simulation and b) grid cells with a statistically significant ($p < 0.05$) change in cold season (Nov–Apr) Q over the period 1981–2010. The change is shaded as a percentage of the 30 yr average for cold season R for that grid. White outlines are basin boundaries for the (west to east) Colville, Kuparuk, and Sagavanirktok rivers.

The Cryosphere Discuss., https://doi.org/10.5194/tc-2019-28
Manuscript under review for journal The Cryosphere
Discussion started: 22 February 2019

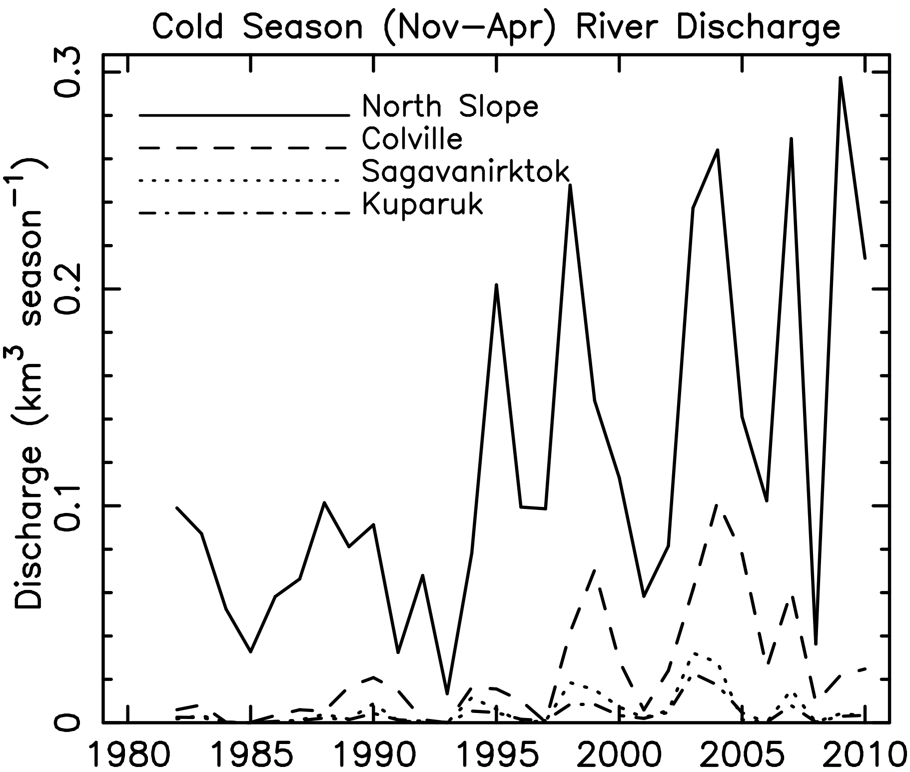

Figure 4: Cold season Q (km^3 season^{-1}) for the full North Slope region and for separately the Colville, Sagavanirktok, and Kuparuk Rivers.

The Cryosphere Discuss., https://doi.org/10.5194/tc-2019-28
Manuscript under review for journal The Cryosphere
Discussion started: 22 February 2019

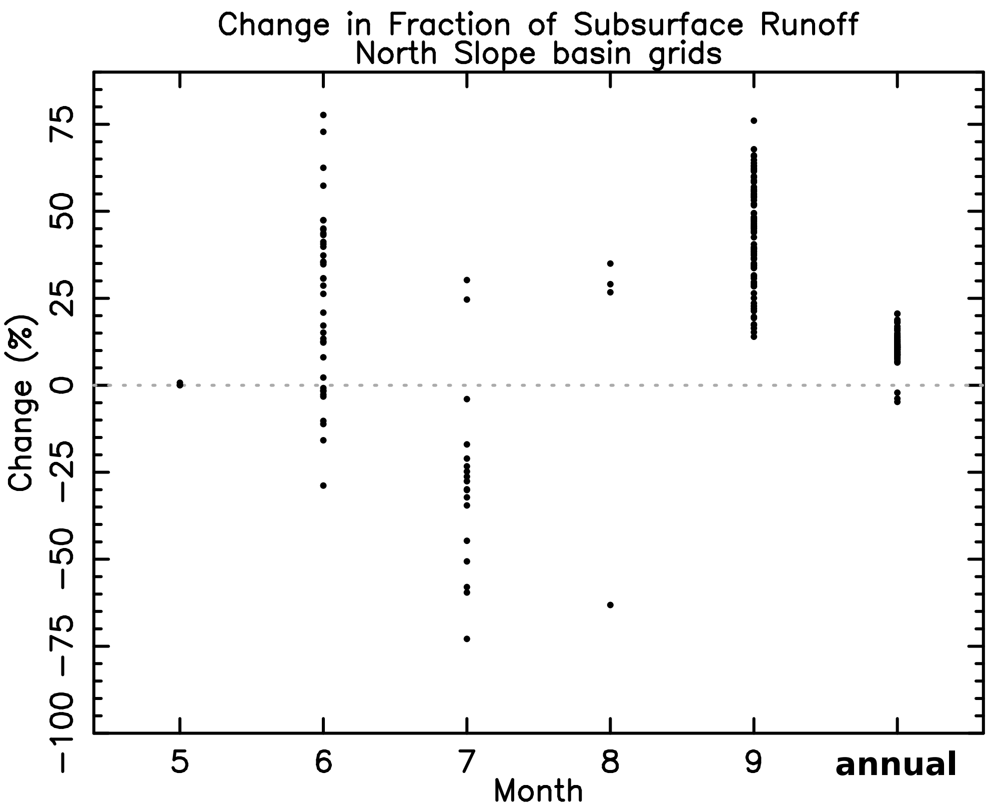

Figure 5: a) Change in fraction of subsurface R (F_{sub}) for warm season months May–September and for annual total F_{sub} and R. F_{sub} changes are not defined for other months due to F_{sub} consistently at 100%, or the grid having no runoff for that month in more than 50% (15 of 30) of the data years. Change is expressed with respect to the long-term average. Dots represent grids that show a significant change at $p < 0.05$. Average for grids with a significant change at the annual scale is +11.0%

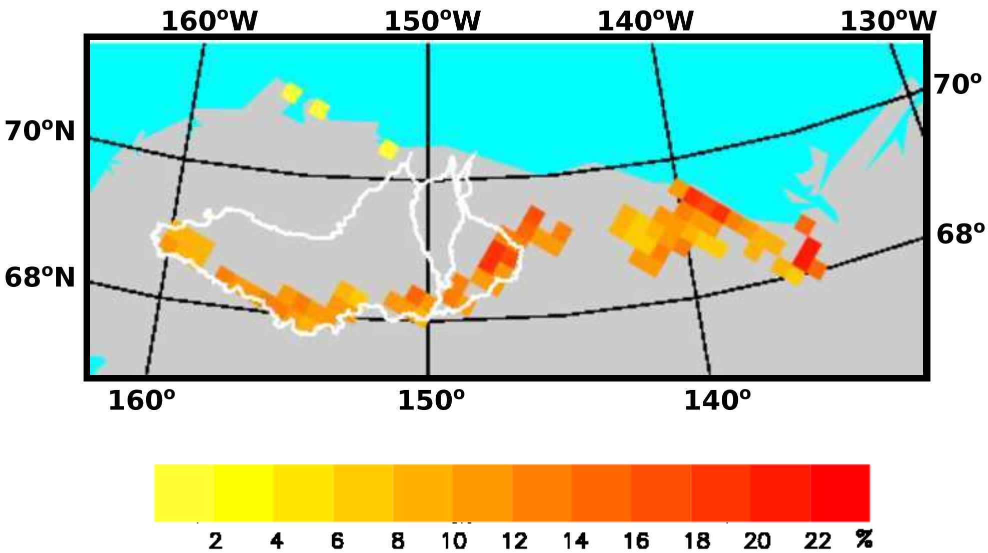

Figure 6: Change in fraction of subsurface R (F_{sub}, %) over the period 1981–2010. Mapped grids show a significant change at $p < 0.05$ based on a two-sided t test.

The Cryosphere Discuss., https://doi.org/10.5194/tc-2019-28
Manuscript under review for journal The Cryosphere
Discussion started: 22 February 2019

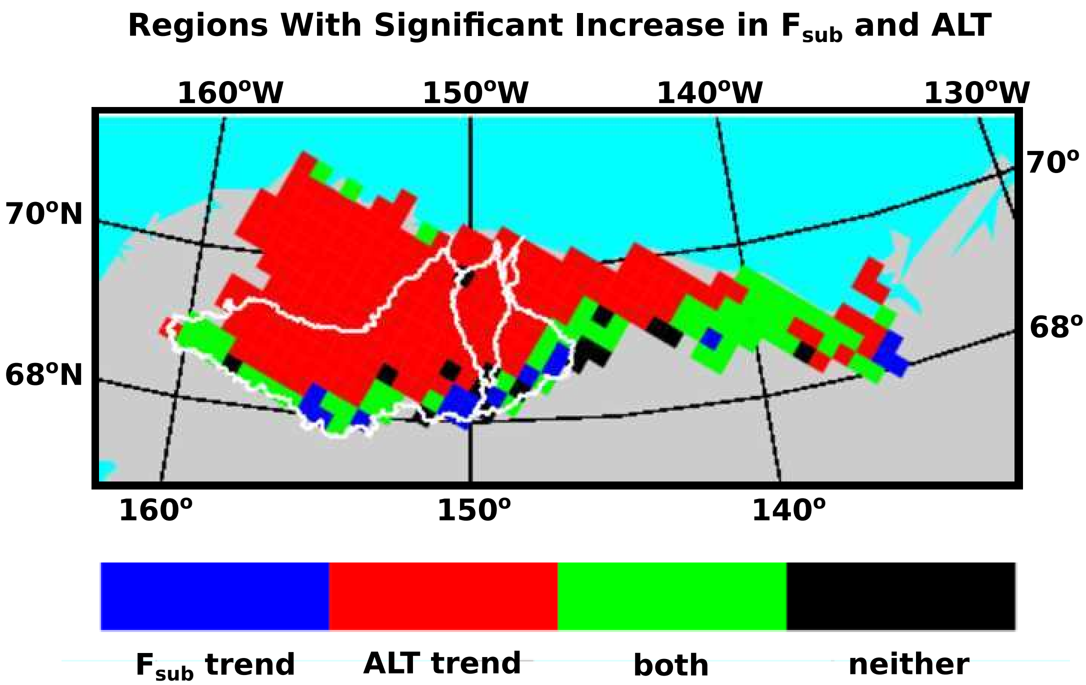

Figure 7: Spatial extent of regions showing a significant increase in annual F_{sub} only (blue), a significant increase in active layer thickness (ALT) only (red), significant increases in both (green), and neither (black). The number of grids, area fraction, and average F_{sub} and ALT increase for each category shown in Table 3.

The Cryosphere Discuss., https://doi.org/10.5194/tc-2019-28
Manuscript under review for journal The Cryosphere
Discussion started: 22 February 2019

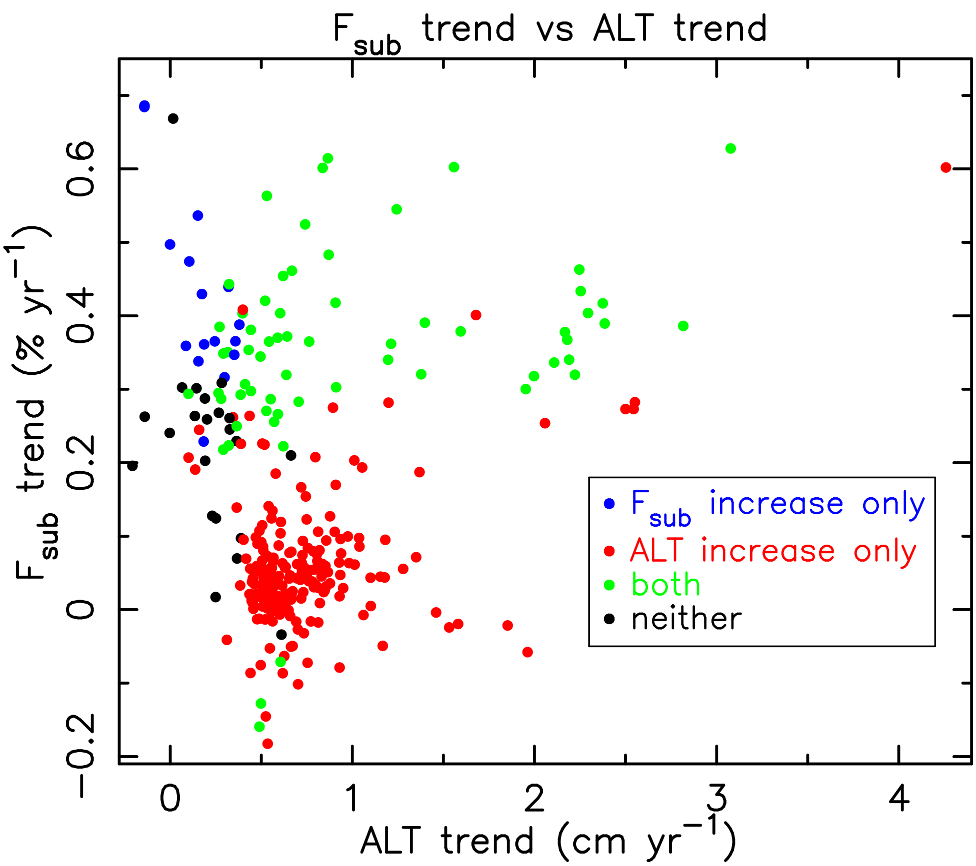

Figure 8: Increase in annual F_{sub} (% yr^{-1}) vs increase in seasonal maximum ALT (cm yr^{-1}) for all 312 domain grid cells. The number of grids, areal percent, and average F_{sub} and ALT increase for each category shown in Table 3.

The Cryosphere Discuss., https://doi.org/10.5194/tc-2019-28
Manuscript under review for journal The Cryosphere
Discussion started: 22 February 2019

The Cryosphere
Discussions
Open Access

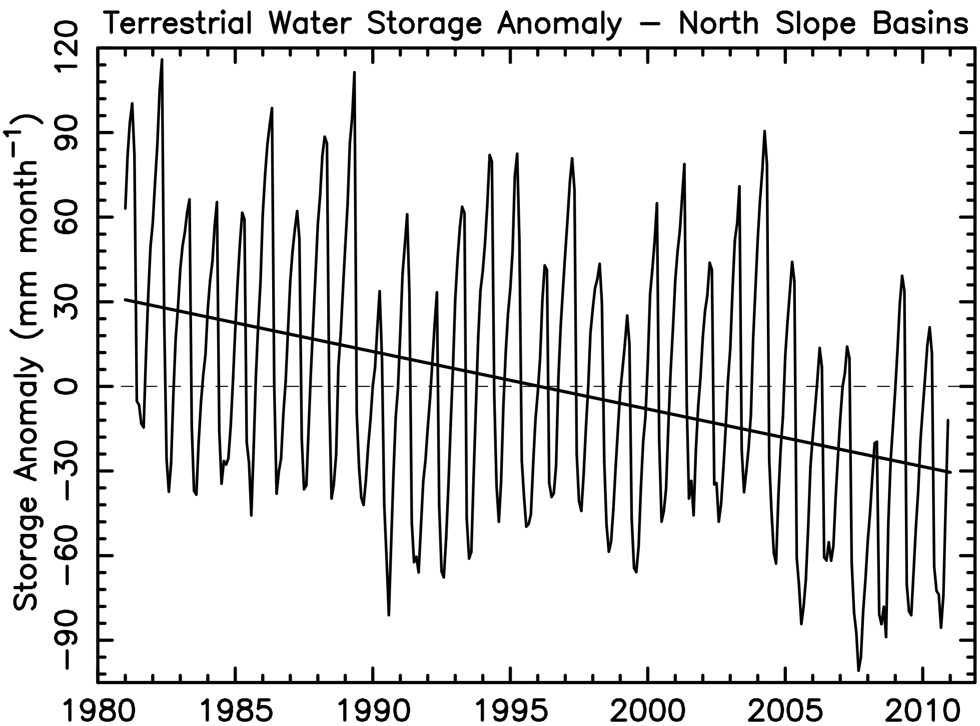

Figure 9: Terrestrial water storage (TWS) anomaly (mm month^{-1}) as an average across the North Slope drainage basin. Anomaly is with respect to the long-term average (1981–2010). In the model TWS includes soil liquid water, ice, and snow storage. It does not include water stored in permanent water bodies such as ponds and lakes.